Annales Geophysicae (2004) 22: 2497–2506
SRef-ID: 1432-0576/ag/2004-22-2497

Annales Geophysicae

The structure of high altitude O^+ energization and outflow: a case study

H. Nilsson[1], S. Joko[1], R. Lundin[1], H. Rème[2], J.-A. Sauvaud[2], I. Dandouras[2], A. Balogh[3], C. Carr[3], L. M. Kistler[4], B. Klecker[5], C. W. Carlson[6], M. B. Bavassano-Cattaneo[7], and A. Korth[8]

[1]Swedish Institute of Space Physics, Kiruna, Sweden
[2]Centre d'Etude Spatiale des Rayonnements, Toulouse, France
[3] Imperial College of Science, Technology and Medicine, London, United Kingdom
[4]University of New Hampshire, Durham, USA
[5]Max-Planck-Institut für Extraterrestriche Physik, Garching, Germany
[6]Space Science Laboratory, University of California, Berkeley, USA
[7]Instituto di Fisica dello Spazio Interplanetario, Roma, Italy
[8]Max-Planck-Institut für Aeronomie, Katlenburg-Lindau, Germany

Received: 29 September 2003 – Revised: 22 April 2004 – Accepted: 1 June 2004 – Published: 14 July 2004

Part of Special Issue "Spatio-temporal analysis and multipoint measurements in space"

Abstract. Multi-spacecraft observations from the CIS ion spectrometers on board the Cluster spacecraft have been used to study the structure of high-altitude oxygen ion energization and outflow. A case study taken from 12 April 2004 is discussed in more detail. In this case the spacecraft crossed the polar cap, mantle and high-altitude cusp region at altitudes between 4 R_E and 8 R_E and 2 of the spacecraft provided data. The oxygen ions were seen as a beam with narrow energy distribution, and increasing field-aligned velocity and temperature at higher altitude further in the upstream flow direction. The peak O^+ energy was typically just above the highest energy of observed protons. The observed energies reached the upper limit of the CIS ion spectrometer, i.e. 38 keV. Moment data from the spacecraft have been cross-correlated to determine cross-correlation coefficients, as well as the phase delay between the spacecraft. Structures in ion density, temperature and field-aligned flow appear to drift with the observed field-perpendicular drift. This, together with a velocity dispersion analysis, indicates that much of the structure can be explained by transverse heating well below the spacecraft. However, temperature isotropy and the particle flux as a function of field-aligned velocity are inconsistent with a single altitude Maxwellian source. Heating over extended altitude intervals, possibly all the way up to the observation point, seem consistent with the observations.

Key words. Magnetospheric physics (Magnetopause, cusp, arid boundary layers; Magnetosphere-ionosphere interactions)

Correspondence to: H. Nilsson
(hans.nilsson@irf.se)

1 Introduction

Since the first report on oxygen ions at plasma sheet energies in the magnetosphere by Shelley et al. (1972) (observation energy range 0.7–12 keV) a number of studies have investigated the energization and outflow of ionospheric origin ions (e.g. Gorney et al., 1981; Yau et al., 1984; Miyake et al., 1993). Energization is typically transverse to the magnetic field and may start just above the ionosphere. The mirror force folds the transversely heated distributions into "conics". For an introduction and recent reviews, see Yau and André (1997); André and Yau (1997); Moore et al. (1999). A particularly important source of upflowing ionospheric ions is the cleft ion fountain (Lockwood et al., 1985) associated with the ionospheric projection of the polar cusp/cleft. The exact relation between ionospheric upflow in the cusp as measured by incoherent scatter radar (e.g. Nilsson et al., 1996; Ogawa et al., 2003) and the more energized ions observed further out in the magnetosphere is still not clear. The further energization of ions of apparently ionospheric cusp origin and subsequent outflow is the subject of several recent studies; Valek et al. (2002) used observations of isotropic magnetosheath-like ions in the dayside magnetosphere (i.e. the cusp) as a spatial reference for observations of upflowing ionospheric ions (of energies up to 450 eV) and could confirm the vicinity of the cusp as the source region. Dubouloz et al. (1998, 2001) used Interball data together with convection estimates and a test particle simulation to backtrace the observed particles and obtain an even better determination of the source region: a 2° latitudinal width region inside the dayside cleft. Some energization was observed to occur up to 10 000 km altitude, though less efficient at higher

altitude. This work has been further extended by Bouhram et al. (2003a, b), who found heating occurring up to 3 R_E. Krauklis et al. (2001) used Polar observations at about 5 R_E altitude to study the acceleration of ionospheric O^+ ions in the cusp low-latitude boundary layer and suggested the two-stream instability as a mechanism for energy transfer from faster flowing H^+ ions to the O^+ ions, based on work by Bergmann et al. (1988); Ludlow and Kaufman (1989). Recent observations further out in the magnetosphere include the observations of very high energy ions of ionospheric origin observed in the cusp by Polar (Chen and Fritz, 2001) and the observations of cold oxygen beams in the tail lobe reported by Seki et al. (1998).

We will complement these studies with Cluster multi-spacecraft studies of high altitude (4–8 R_E) ion outflow over the polar cap, mantle and high-altitude cusp. The energies reported in the above cited papers tend to increase with observation altitude, consistent with heating over extended altitude intervals, as inferred by Miyake et al. (1993); Bouhram et al. (2003b). However, it is an important question as to how much further energization takes place at high altitude. We will try to test both the assumption of a "single source altitude", which means that most heating/acceleration takes place well below the spacecraft, and the assumption that we have heating over extended (though not necessarily continuous) altitude intervals. For the likely case of an upstream source any outflow related structures should be brought from the source by the convection and we will use multi-spacecraft correlation techniques to see if this is the case. We will also examine the correlation data to see if anything can be said about scale-sizes of structures using the rather small spacecraft separation distances.

2 Measurement technique

We use data from the Cluster Ion Spectrometers (CIS) on board Cluster II spacecraft 1, 3 and 4. The CIS instrument is described in detail in Rème et al. (2001). CIS consists of two different ion spectrometers, Composition Distribution Function (CODIF), which can resolve the major magnetospheric ions, and Hot Ion Analyzer (HIA), which has no mass resolution but higher angular and energy resolution. We will only present results from the CODIF instrument.

CODIF can resolve H^+, He^{++}, He^+ and O^+ through a time-of-flight technique. The detector has a field-of-view of 360° orthogonal to the spin plane, divided into 16 sectors of 22.5° each. The angular resolution is likewise 22.5° in the spin plane. The energy coverage in the modes of interest to us is from 15 eV per charge up to 38 keV per charge, in up to 30 logarithmically spaced steps with a $\Delta E/E$ of 0.16. Furthermore, we use data from the Cluster fluxgate magnetometers (Balogh et al., 2001).

3 Data analysis technique

The analysis of multi-spacecraft data is discussed extensively in Paschmann and Daly (1998). For the ion data discussed here we compare moments of the distribution function through cross-correlation of the time series from the different satellites. This can primarily yield the phase delay between the spacecraft but possibly also some information on spatial scale sizes and/or time lags over which a good correlation can be found.

3.1 Cross-correlation of multi-spacecraft data

Our primary aim with a cross-correlation is to find out if structures seen with the different spacecraft have similarities (high correlation) and to determine the phase delay for maximum correlation. The data from the spacecraft are resampled with the average time separation of the data points in the interval around 4 s (one spin). From each data set N data points are picked out, with a successive displacement of the second data-set relative to the first. The number of points being cross-correlated is thus N for all relative displacements. Furthermore, any data gaps are interpolated. The larger the parameter N, the less noise sensitive the estimate will be, but also vulnerable to phase delay changes on the $N \times t_{\text{resample}}$ time scale. In our analysis we found that 160 samples (about 10 min) was a good compromise. Smaller windows gave consistent but more noisy results.

3.2 Estimating phase-delay due to convection

To determine the delay time we assume a locally plane structure extending orthogonally to the convection and along the field-line, which yields the delay time as

$$t_{\text{delay}} = \frac{\boldsymbol{r_2} - \boldsymbol{r_1}}{|v_c|^2} \cdot \boldsymbol{v_c}, \tag{1}$$

where $\boldsymbol{r_1}$ and $\boldsymbol{r_2}$ are the position vectors for the spacecraft and $\boldsymbol{v_c}$ is the field-perpendicular plasma drift vector obtained from the CIS O^+ moment of the first spacecraft, assumed to be constant on the time scale of the lag between the spacecraft. The assumption about a plane structure is necessary but it can easily be tested a posteriori, since the cases when the spacecraft separation is along the convection are independent of this assumption. The position of the second spacecraft should be for the time when the front actually arrives, making it either a recursive problem or dependent on the phase delay calculated from the cross-correlation results.

3.3 Estimating the source region

As ionospheric particles are energized and flow outward in the magnetosphere they are also brought from the source region by the convection. For the cases we are studying convection was antisunward over the polar cap. Figure 1 illustrates the path of a number of particles emanating from a source region with a finite spatial width in the direction of the flow, i.e. each convecting field-line will experience the source for a limited time.

Particles with a high field-aligned velocity will reach a high altitude (y-axis) quickly (line to point 1 in Fig. 1 represents highest velocity observed). The observed change in

the parallel velocity with time can be used to estimate the distance to the source region along the field line, S_d. This and all other variables mentioned below are illustrated in Fig. 1. The estimation of the time for convection to bring a field-line from one spacecraft measuring position to the next is analogous to the discussion in the previous section, except that we use consecutive locations of the same spacecraft instead of two different spacecraft. We can thus calculate a $t_{\rm delay}$ according to Eq. (1) for our satellite trajectory and sum up the result as a "convection time", t_c. After a time t_c' (x-axis of Fig. 1) we expect to see particles with a field-aligned velocity $v_\parallel$ of S_d/t_c', where $t_c' = t_c + t_0$ and t_0 represents the initially unknown convection time between the source and the start of our observations. The field-aligned velocity $v_\parallel$ and the convection time t_c are obtained from our measurements, so that S_d and t_0 can be estimated. This is done through a first order least-square fit of $v_\parallel^{-1}$ to t_c. In practice, as we observe the ion beams for several hours, it is necessary to take the increased altitude of the spacecraft into account as well. The time it takes the particles to travel the increased altitude ($\delta alt/v_\parallel$, where δalt is the difference between the observation altitude and the minimum altitude of observations used for the fit) is subtracted from the estimated convection time.

The range of different slopes which can be drawn from an observation point (e.g. point 2 in Fig. 1) to the source represents the range of velocities which can be observed. Analytically, this can be expressed as

$$\Delta v_\parallel = \frac{\Delta t \cdot v_\parallel^2}{S_d}, \tag{2}$$

where Δt is the source size in time units (Fig. 1) which can also be described as the residence time of the ions in the source region. As this expression describes which particles can be observed, it will determine the parallel temperature if the velocity range $\Delta v_\parallel$ is small compared to the range of velocities emanating from the source.

When particles are moving up a field-line, the mirror force will act to conserve the magnetic moment, thus changing transverse energy into field-aligned until essentially all kinetic energy is in the field-aligned direction (the upward folding of a "conic"). This means that the fit achieved in the above discussion is an underestimate of the source altitude, as the particles will have had a lower field-aligned velocity during part of their journey. This is also true if the particles have passed through a field-aligned potential drop. In principle one may take the mirror field into account analytically or release random non-interacting particles in a mirror field in a simple code and make the above fit to the model where the start altitude is adjusted until the fitted altitudes agree.

The result thus obtained assumes a single source altitude, a constant position of the source region and no dependence on the spacecraft motion orthogonal to the flow. The first limitation is something we want to test so that is not a problem. The importance of the other two limitations is described in Fig. 2, and also discussed in Dubouloz et al. (1998). Essentially, if the convection is entirely along the spacecraft

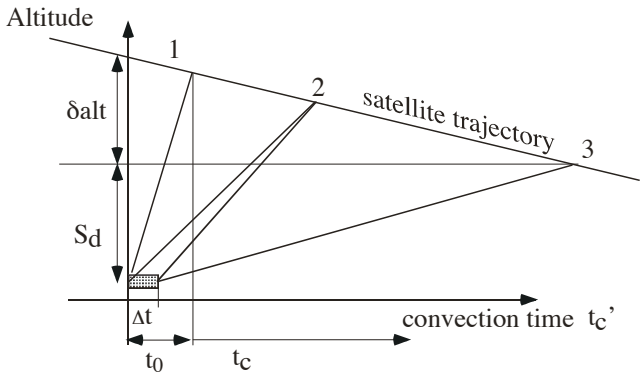

Fig. 1. Illustration of particle trajectories for particles with different velocities emanating from a finite low altitude source region. The x-axis shows the time the particle has been convecting away from the source, which for constant convection would be a distance scale. The point labeled 1 indicates the fastest particles which are thus observed furthest upstream. All trajectories between the two indicated trajectories reaching point 2 represent the velocities (i.e. different slopes) which can reach that observation point from a source of finite extent (if particles with that velocity exist). At point 3 the extent of the source region is less significant and the range of observable velocities small.

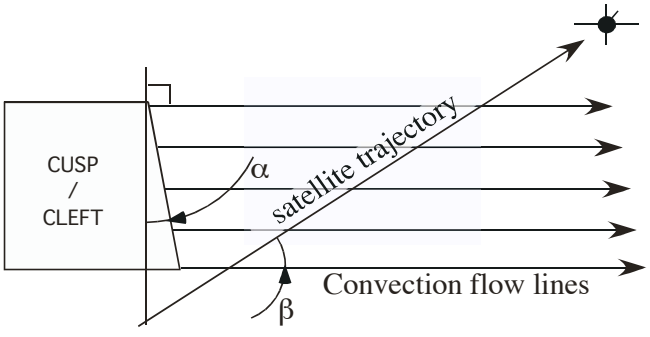

Fig. 2. Illustration of the satellite trajectory orthogonal to the plasma flow. The important parameters defining the uncertainty in a velocity dispersion analysis are the angles α (flow – source angle) and β (spacecraft trajectory – flow angle).

trajectory (β=0°, where the angle β is defined in Fig. 2), it does not matter if the source is extended orthogonally (angle α as defined in the figure is 0°) to the flow or if there is any other variation along the the distribution of the source orthogonally to the flow. Approximately the uncertainty due to a finite α will be $S_d \cdot \tan\alpha \cdot \tan\beta$, from geometrical considerations (Fig. 2, S_d scale with distance downstream).

3.4 Parallel to perpendicular temperature ratios

As discussed in the previous section the velocity dispersion effect will determine the range of parallel velocities which can be observed from a single altitude source and influence the range of velocities seen above any source in the same way. The mirror force will transfer energy from the

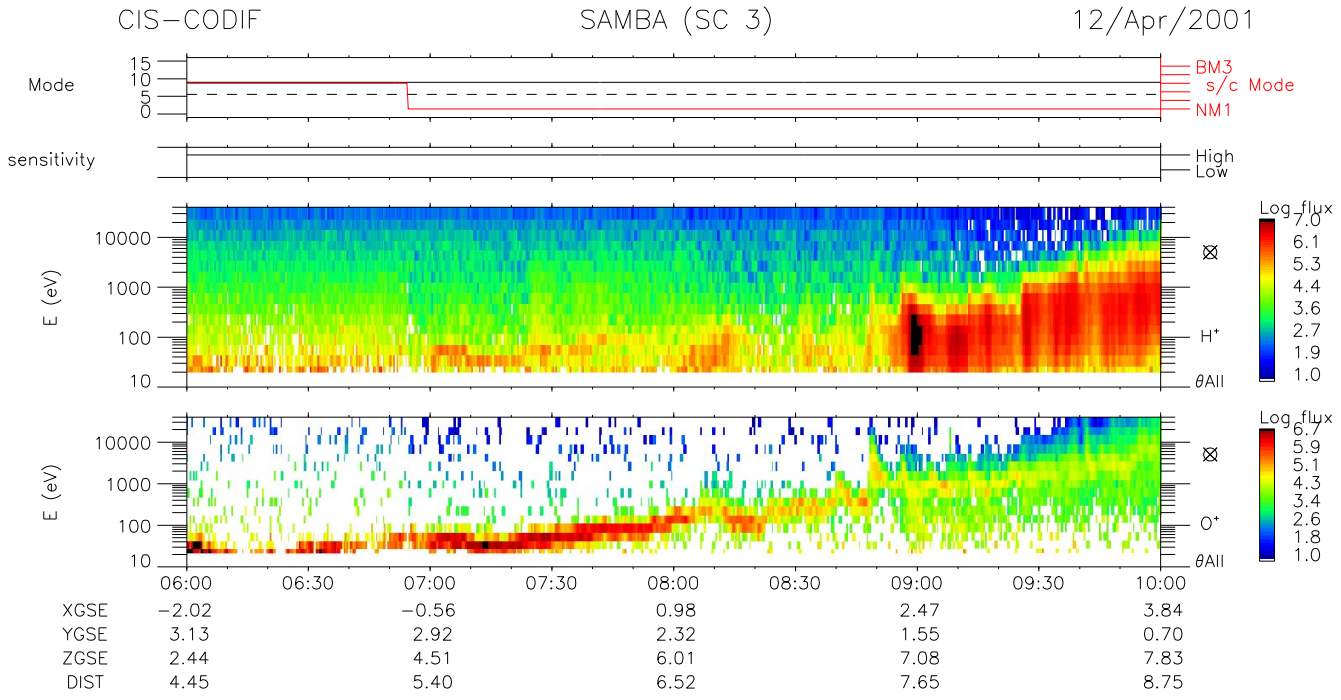

Fig. 3. Cluster spacecraft 3 (Samba) data from 12 April 2001. Panel 1 shows spacecraft mode, panel 2 instrument mode. Panels 3 and 4 show the H^+ and O^+ energy spectrograms, particle flux integrated over all directions.

transverse to the parallel direction, thus affecting both the parallel and perpendicular temperature in a predictable way (i.e. the "folding" of the conic distribution). In practice, a certain part of the conic will be seen (determined in the case of a limited distant source by the velocity dispersion) and the expected temperature ratio will not only be determined by the change in the magnetic field. For our discussion it suffices to note that the mirror force will decrease the transverse energy at high altitude and also decrease the ratio of the transverse to parallel velocity ranges with the upward folding of the conic. The velocity dispersion will decrease the range of observed energies with travel time from the source (Eq. 2, travel time=$S_d/v_\parallel$).

3.5 Effect of heating from a source extended in altitude

To complement the discussion in the previous section we here consider a simple estimate of what field-aligned outflows can be expected from transverse heating over an extended altitude interval. A very useful order of magnitude estimate is to assume that the perpendicular energy of the ions is held constant as they flow outward into weaker magnetic field regions, despite the mirror force. This leads to a particularly simple expression for the field-aligned flow as a function of the observed perpendicular energy;

$$\begin{aligned} v_\parallel(z_{\max})^2 &= v_\parallel(z_{\min})^2 + \int_{z_{\min}}^{z_{\max}} \frac{dB}{dz}\frac{1}{B} v_\perp^2 \, dz \\ &= v_\parallel(z_{\min})^2 + [ln(B(z_{\min})) - ln(B(z_{\max}))] v_\perp^2, \end{aligned} \quad (3)$$

where $z_{\min}$ and $z_{\max}$ are the minimum and maximum of the altitude range over which the calculation is performed. This estimate ignores the curvature of the field lines and the associated effect on parallel acceleration, e.g. the centrifugal force (Cladis, 1986). With this simple expression one can estimate if it is feasible to assume that the observed parallel kinetic energy has been transferred from extended transverse heating of the particles. We will assume that the perpendicular energy has been kept constant at the thermal velocity of the observation altitude from the lowest altitude used in our estimate, i.e. assuming the temperature is a function of distance downstream only. This assumption is used solely for simplicity.

4 Observations

The case discussed in this paper has been picked out among a number of several keV energy oxygen beams observed by the Cluster II satellites in spring 2001. For this time period the Cluster spacecraft crossed the dayside magnetopause and polar cap at high altitude. The events are rather striking from the energy spectrograms, last several hours (appear limited by spacecraft position rather than the lifetime of the structures) and appear to be fairly common (though a statistical study is a future project). Of these days 12 April 2001 was chosen for a correlation and velocity dispersion study to complement the detailed single spacecraft report on this event by Joko et al. (2003a)[1].

[1] Joko, S., Lundin, R., Nilsson, H., Sandahl, I., Rème, H., Bosqued, J.-M., Sauvaud, J.-A., Dandouras, I., Möbius, E., Kistler, L. M., Klecker, B., Carlson, C. W., McFadden, J. P., Parks, G. K.,

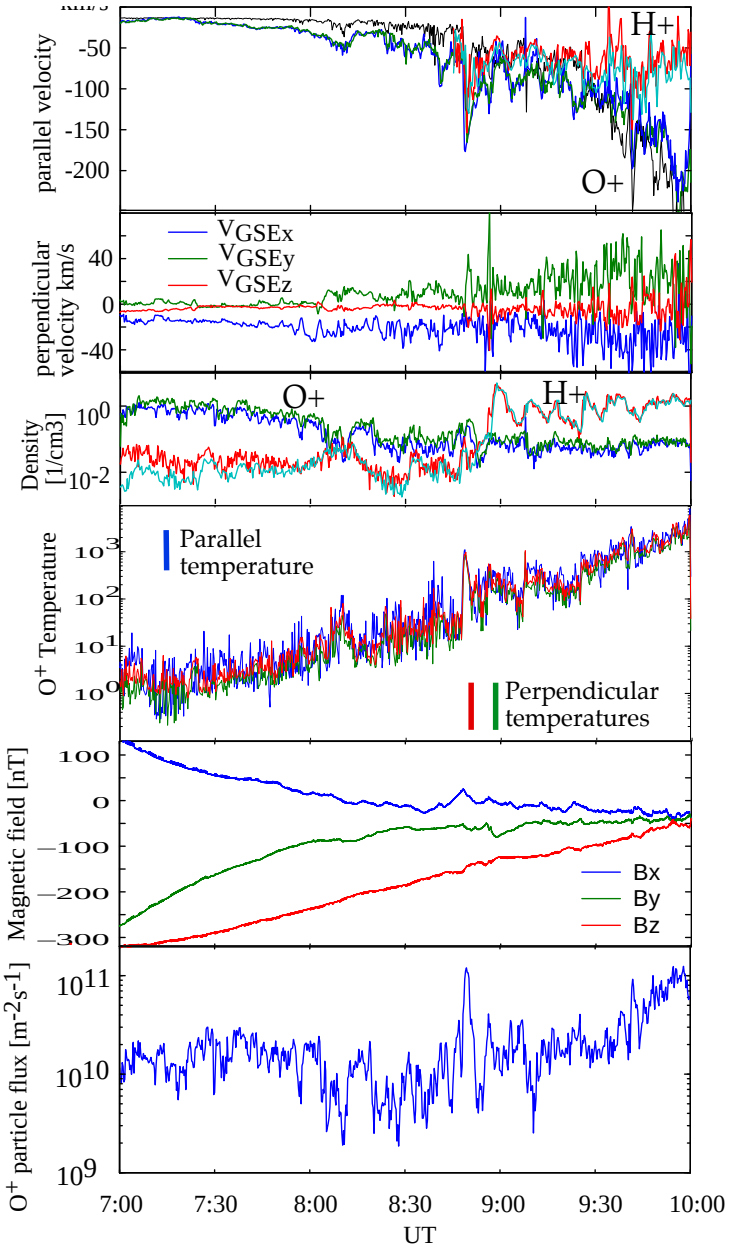

Fig. 4. Moment data for spacecraft 3 (unless otherwise mentioned). Panel 1 shows the field-aligned velocity (positive in the direction of B), where red and cyan show H^+ from spacecraft 3 and 4, respectively, and blue and green show O^+ for spacecraft 3 and 4. Also included is a simple estimate of the parallel velocity (thin black line, see text for details). Panel 2 shows the field-perpendicular velocity panel in GSE coordinates (blue, green, red are x, y, z coordinates, respectively), panel 3 the density (same colour code as parallel velocity), panel 4 the parallel and perpendicular temperatures for O^+, panel 5 the magnetic field components and panel 6 the O^+ number flux normed with the magnetic field strength at 07:00 UT.

The IMF for the time period showed a dominant B_y of -20 nT, and a variable B_z of about -8 nT before 07:00 UT (at ACE spacecraft) and then about 0 nT, except for an excursion to -5 to -10 nT between 08:10 and 08:20 UT. This excursion was coincident with a dynamic pressure increase from 0.5 to 3.5 nPa. Average solar wind velocity was 650 km^{-1}, yielding an approximate delay time from ACE of 36 min. Data were available from spacecraft 3 and 4. Energy spectrograms of H^+ and O^+ from spacecraft 3 are shown in panels 3 and 4 of Fig. 3. The moments are summarized in Fig. 4, from spacecraft 3, obtained at altitudes between 3.4 and 7.8 R_E.

Panel 1 shows the field-aligned (parallel) velocity (positive in the direction of the magnetic field, i.e. for injected particles) of H^+ (red spacecraft 3, cyan spacecraft 4) and

Bavassano-Cattaneo, M. B., Korth, A., and Eliasson, L.: Outflowing O^+ ions at high altitudes in the dayside magnetosphere observed by CIS/Cluster, Case study: April 12, 2001, Ann. Geophys., submitted, 2003a.

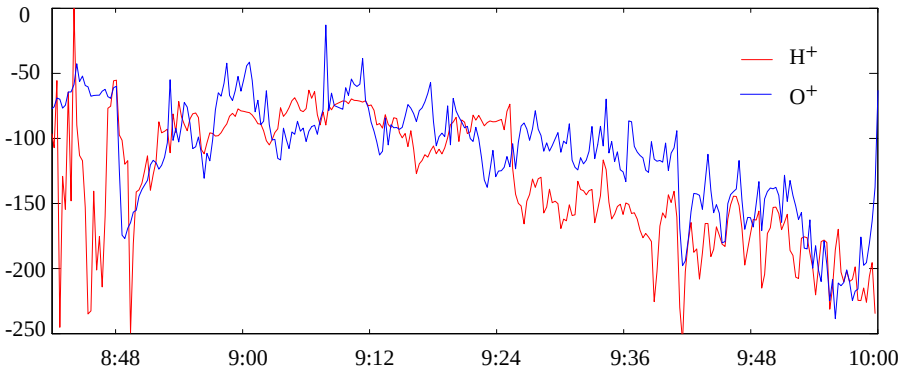

Fig. 5. Parallel velocity for O^+ (blue) and H^+, calculated for upward moving particles only (red).

O^+ (blue spacecraft 3, green spacecraft 4), panel 2 the field-perpendicular velocity of O^+ (GSE coordinates, blue, green red for x, y, z, respectively), panel 3 the density of H^+ and O^+ (same colour code as parallel velocity), panel 4 the parallel and perpendicular temperatures, panel 5 the magnetic field which shows that the spacecraft was well inside the magnetosphere and panel 6 shows the O^+ number flux normed with the magnetic field strength at 07:00 UT to take into account the widening of the flux tube. Also shown in panel 1 of Fig. 4 is the simple estimate of the parallel velocity of O^+ resulting from extended transverse heating (black line), as described in Sect. 3.5. Noteworthy features are the increase in the oxygen ion energy with altitude and/or time, which may also be interpreted as distance upstream as the convection is antisunward. The O^+ energy spectrogram is wider in the region with magnetosheath plasma (after 09:00 UT, also seen in the temperature estimates), widening also for energies below the peak flux. For velocity dispersion from a source with a distinct onset there should be a relatively sharp cut-off at the energy of the slowest particles which reach the observation point. The number flux does not show a clear trend, but increases somewhat at the highest energies and/or altitudes in the upstream direction. This is not consistent with the flux from a single Maxwellian source of any temperature.

Both O^+ and H^+ show a net outflow. The O^+ ions increase their energy with time in a manner very similar to the upper energy cut-off of the protons, but at somewhat higher energies. In Fig. 5 we compare the parallel velocities of the two ion species when the H^+ moment is calculated for upward moving particles only; the two velocities are now much more similar. We show here only the H^+ data after 08:48 UT when there is a significant flux of H^+. This H^+ outflow cannot be separated into ionospheric and mirroring magnetosheath ions. Finally, we note that at the highest altitudes some high-energy O^+ are also seen in the downgoing direction, associated with partial shell-like distributions (described in Joko et al., 2003b). This seems to be associated with processes at an even higher altitude and will not be further considered here.

Concerning the O^+ temperature one may note that the ions are essentially isotropic (Fig. 2, panel 4, where blue is parallel, and red and green perpendicular temperatures) with a noisy deviation from isotropy. Cross-correlating the parallel to perpendicular temperature ratio yields very low correlation between the two spacecraft (not shown).

We now turn to the cross-correlation of the rest of the data from this event. The relative position of spacecraft 3 and 4, defined as spacecraft 3 position minus spacecraft 4 position, was, on average, (GSE coordinates) (687, −391, 448) km during the event. Figure 6 shows the correlation coefficient (panels labeled a) and phase delay for maximum correlation (red crosses in panels labeled b), along with the expected phase delay due to convection (solid black line) and field-aligned outflow (green line). Positive phase delay means that the structure is seen first at spacecraft 3. The cross-correlated parameters are for panels 1 O^+ field-aligned velocity, panels 2 magnitude of O^+ field-perpendicular velocity, panels 3 O^+ logarithm of density and panels 4 the high-pass filtered (period below 26 min to remove the background magnetic field) magnetic field components. Blue line crosses show B_x results, green B_y and red B_z, respectively. The cross correlation window size was 160 lags with 4-s resolution, i.e. about 10 min. As can be seen the phase delay for the field-aligned velocity and the density agree well with what can be expected from convection. The spacecraft motion in the direction of convection is at most 10% of the convection and ignoring it does not significantly affect the result. The delay time range from 10 to 60 s, which is not a major problem for our assumption that convection, was locally constant. The perpendicular drift shows close to zero phase delay, also if it is subdivided into flow along and perpendicular to the spacecraft separation vector. The components of the magnetic field show an excellent agreement with what is expected from convection most of the time. Notable are the periods with zero delay in the magnetic field components, in particular at around 08:50 UT. The latter case corresponds to a heating outflow event clearly seen also in Fig. 4 and discussed in more detail in Sect. 5.3. Convection was antisunward (against satellite motion) so that early measurements were downstream; (Fig. 4), panel 2. In the upstream region there was a strong dawnward component, as can be expected from the IMF conditions. It is thus possible that the entire observed structure was caused by energization in a small region somewhat upstream of the

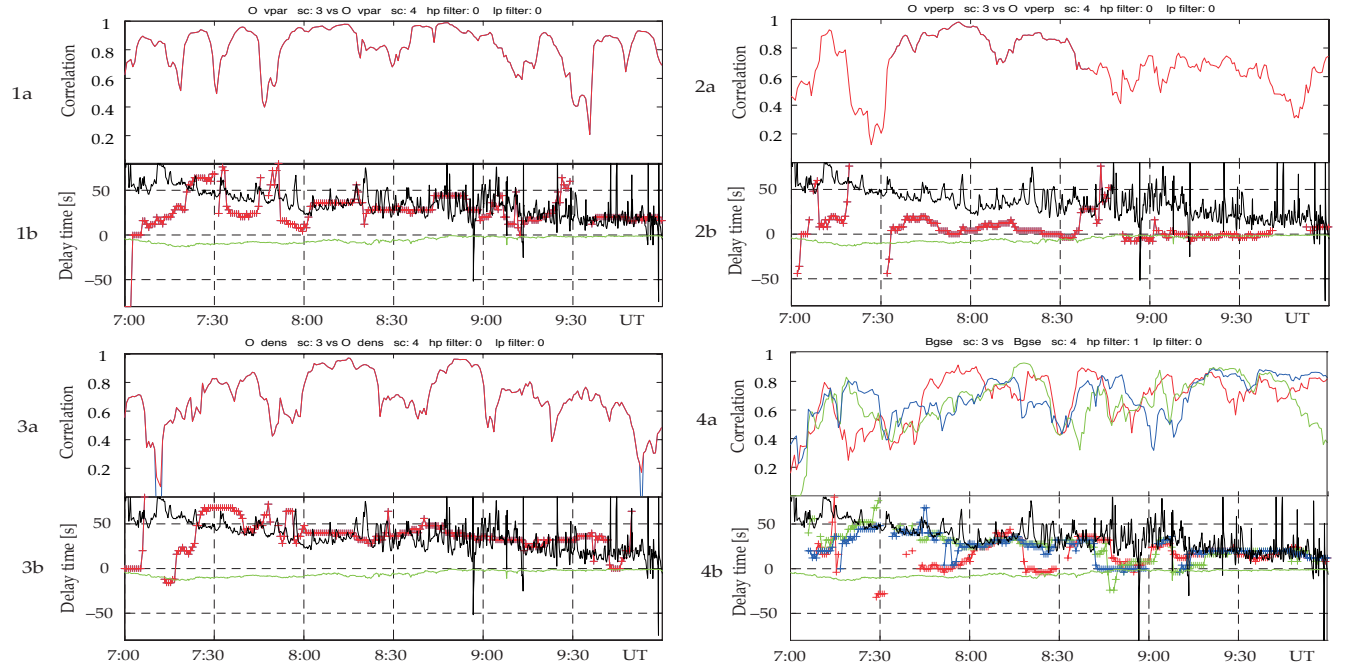

Fig. 6. Cross-correlation results with spacecraft 3 leading spacecraft 4. The correlation window was 160 lags (approximately 10 min). The **(a)** panels show cross-correlation coefficients, whereas the **(b)** panels show time delay for maximum correlation (red crosses), the time delay expected due to convection (black line) and field-aligned flow (green line). Panels 1 show correlation results for O^+ parallel velocity, 2 perpendicular velocity, and 3 density. In panel 4a is shown the correlation coefficient for the magnetic field components, blue is for B_x, green B_y and red B_z (GSE coordinates). Panel 4b uses the same colour code for the delay time.

highest energy ions observed, and well below the lowest altitude of observations, as discussed in Sect. 3.3. Fitting $v_\parallel^{-1}$ to $t_c - \Delta alt/v_\parallel$ yields an estimate of the source altitude of about $1.5R_E$ altitude. Using $v_\parallel \pm 1/2 v_{T\parallel}$ yields $\pm 0.5R_E$ in the fit result ($v_{T\parallel}$ is the thermal parallel velocity). A further test of the velocity dispersion scenario can be made by investigating $v_{T\parallel} S_d / v_\parallel^2$ (see Sect. 3.3, $v_{T\parallel}$ is a measure of the range of parallel velocities observed) which is an estimate of the source region size measured in seconds. This value is rather noisy but centered around 400 s. Using this value and the values from the least-square fit, which yielded source distance and a time offset (the constant of the fit), as well as the altitude change of the spacecraft, one can reconstruct the expected parallel energy spectrogram time series and achieve a good similarity with observations. The upstream high altitude data closer to the source (in time, not altitude) is predicted to be hotter in parallel temperature compared to the low altitude downstream data (as observed), but the relative perpendicular temperature should be lower due to the mirror force (i.e. upward folding of the conic). Finally, we note that the angle β as defined in Fig. 2 was, on average, 31° between 07:00 and 10:00 UT for spacecraft 3 and thus fairly well suited for this type of estimate. If we arbitrarily choose α=15° (Sect. 3.3), we obtain a consistent source distance error of 0.5 R_E, indicating that this uncertainty is large but not a major problem.

Further information can be gained from a detailed study of the mesoscale O^+ heating and outflow events which occur; a particularly clear example can be seen at 08:48 UT, reproduced in detail in Fig. 7. This is the first case of clear broadening of the energy spectra and represents a sudden increase in the outflow velocity. The sudden onset and subsequent decay with time (and further upstream) is inconsistent with velocity dispersion. To obtain lower velocities further upstream in the velocity dispersion scenario the source must move downstream. The temperature is isotropic. An inspection of both spacecraft data shows that they did not encounter the outflow/heating event at the same time. The sharp onset is thus a spatial feature. The event appears related to a sudden change in IMF B_z, beginning at 08:10 UT at the ACE spacecraft.

5 Discussion

5.1 Correlation results

The observed structures are readily explained by structures drifting with convection. The only exception is the perpendicular ion drift, where it is reasonable that changes are propagating along the magnetic field as Alfvén waves. There are also some cases where there seems to be no phase delay in the components of the magnetic field and one such case is discussed in Sect. 5.3. We have also investigated the correlation coefficient as a function of time delay for maximum correlation and as a function of distance between the spacecraft along the assumed propagating front. Neither show any correlation. The latter means that the structures are typically larger than the spacecraft separation distance but have sharp enough borders that low correlation is sometimes obtained

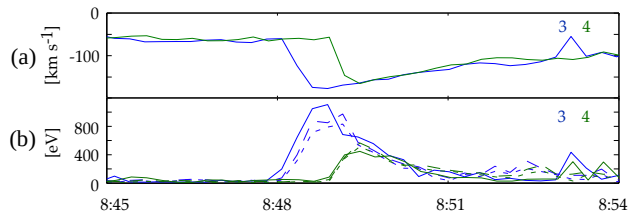

Fig. 7. Detailed plot of data from a mesoscale heating event. Panel **(a)** shows the field-aligned velocity for O^+ for spacecraft 3 and 4. Panel **(b)** shows the parallel and perpendicular temperatures measured by the same satellites (solid line is parallel temperature).

also for small separations in time and space. The lack of dependence on delay time means the same but for field-aligned scale sizes.

5.2 Structure of outflowing ions and of the source region

The oxygen ion structures reported here show a number of features which can tell us something about the source region. The main features are:

1. A significant flux is seen mainly in a narrow energy range. The mean energy and range of observed energies (temperature) increase with altitude, distance and/or in the upstream flow direction. The kinetic energy is dominated by the field-aligned velocity.

2. The O^+ field-aligned velocity is approximately equal to that of H^+ when the latter is calculated for outflowing ions only.

3. Heating and/or acceleration is continuous for at least several hours in the sense that no "holes" in the ion structure (i.e. absence of outflowing particles) are observed, i.e. all field-lines experience heating/acceleration.

4. The outflow structures are drifting with convection at the altitude and time of observation, though mesoscale events may show temporal change.

5. The O^+ temperature is essentially isotropic.

6. The number flux shows no clear trend, except for an increase at the highest altitude and/or energy.

Item 1) tells us that the source (energization region) must be limited in time for each field line or an acceleration process with little heating. There are three ways to explain the large-scale O^+ energy structure; (i) velocity dispersion from a limited heating region well below the spacecraft where the velocity dispersion yields the limited energy range (though one then expects a rather sharp low-energy cut-off which is not observed in the hotter high-altitude part); (ii) altitude dependent heating/acceleration and/or (iii) distance downstream dependent heating/acceleration. If it is transverse heating, it must be well below the spacecraft as the field-aligned kinetic energy dominates, or gradual heating over extended altitude intervals. As the magnetosheath H^+ population is initially hotter and reasonably faster flowing than the ionospheric O^+ population, item 2) indicates that the heating and acceleration mechanism is more efficient for the heavier and/or colder ions or takes place where the magnetosheath H^+ ions are not affected (i.e. below their mirror altitude or a field-aligned potential drop). Outflow with the same velocity for both species may indicate energization up to the same velocity (though it is not clear if H^+ is energized at all). Concerning the possibility of a field-aligned potential drop as the acceleration mechanism, item 2) shows that this cannot operate on both ion species, as H^+ should then attain a higher velocity than O^+. However, the magnetosheath plasma may have entered the potential drop from above and been reflected, ending up unaffected, though then we cannot explain the approximate similarity. Items (1), (3) and (4) are consistent with a cusp related source, as even if the cusp is intermittent and bursty, any new cusp flux added to the polar cap will be added just adjacent to the previous bundle (assuming dominating B_z negative or strong B_y conditions). The velocity dispersion analysis and the fact that the flow was essentially antisunward as well as the presence of the magnetosheath-like plasma further strengthen the arguments for a cusp-related source. Item 4) in itself is a necessary (but not sufficient) condition for an upstream (not local) source. Item 5) tells us that velocity dispersion from a single altitude cannot explain our observations. Nor can we identify the two-stream instability as a mechanism of energy transfer from H^+ to O^+ using temperature anisotropy, as was discussed in Krauklis et al. (2001) (nor exclude it). Item 6) finally points further towards gradual heating acceleration rather than a strong heating event in a limited altitude interval (assuming this yields a Maxwellian distribution), though not necessarily up to the observation altitude. However, a careful examination shows that a bi-Maxwellian distribution of a cold (thermal velocity 30 km/s) and a hot (of the order of magnitude of the highest flows, i.e. 200 km/s) is consistent with the observed number flux as a function of particle velocity.

Heating over extended altitude intervals as reported in Bouhram et al. (2003b) is essentially consistent with the observations, as further indicated by the simple estimate we performed according to the scheme described in Sect. 3.5. In general, one can adjust the parallel to perpendicular temperature ratio by releasing particles at several altitudes instead of over an extended time. This allows for a change in the relation between parallel and perpendicular temperature, and one may possibly use this for a more advanced velocity dispersion analysis. However, such simulations should be performed with a proper model, such as that of Bouhram et al. (2003a), allowing for a proper description of the heating. That model is currently limited to altitudes up to 3 R_E, but for the case of 12 April 2001 that could explain much of the observations.

5.3 Mesoscale heating event

The mesoscale heating event at around 08:50 UT described in Sect. 4 and shown in detail in Fig. 7 appears to be a structure drifting with convection according to the particle correlation results. The magnetic field component correlation analysis indicates no time delay for this event. The particle structures are very heavily influenced by the sharp poleward border, whereas there is very little structure otherwise. Indeed the values of the field-aligned velocity and temperature are the same at the same time for both spacecraft once they are both within the heating/outflow region. This leads to the very straightforward conclusion that we are observing the temporal decay of a heating outflow event within a region with a sharp poleward border. The velocities observed are thus not determined by velocity dispersion from a distant source. The sharp poleward border then indicates a spatially limited cusp transient event, possibly triggered by a southward turning IMF and or dynamic pressure increase occurring 38 min earlier at ACE, consistent with the expected time delay between ACE and the Earth.

6 Conclusions

The data studied in this paper indicate that the observed O^+ ion outflow emanates from the cusp region, thus constituting an energized high-altitude extension of the cleft ion fountain. A velocity dispersion and multi-spacecraft correlation analysis indicate that a source well below the spacecraft is consistent with the data. However, the parallel to perpendicular temperature ratio is not consistent with a "single" altitude source, where single altitude means a small source compared to the travel distance to the observation point. Heating of O^+ over extended altitude intervals is consistent with all our data. Most of it will then take place below and upstream of the observations. It is thus worthwhile for future studies that also include wave data to try to identify waves involved in particle acceleration and heating in the altitude region above $4R_E$, as well as waves associated with pitch-angle diffusion, as this affects the observed temperature ratios and their interpretation.

The parallel bulk velocity of O^+ is approximately the same as that of H^+ and the highest energy with a significant flux of H^+ is typically below the energy of peak O^+ flux, both consistent with the observations of Seki et al. (1998). The energy of the two ion species appears coupled, though the details of this coupling remain to be studied. We could neither confirm nor reject a two-stream instability, though it seemed not likely to take place at the observation site. Another possibility is a heating and/or acceleration mechanism which is more efficient for the colder and heavier population, such as the ponderomotive force (Guglielmi and Lundin, 2001), which could yield acceleration up to the same velocity for the two species. We suggest that the ions reported here are a viable source for the tail lobe mantle O^+ beams reported by Seki et al. (1998), consistent with one of their suggested supply routes.

The correlation data also allowed us to tentatively identify the temporal decay of a mesoscale heating/outflow event with a sharp spatial border. The correlation coefficient variations indicated that structures observed were typically larger than the spacecraft separation but with sharp borders which also allowed for low correlation for small separation in time or along an assumed convection front.

Acknowledgements. The work of HN, SJ and RL was supported by the Swedish Space Board. We thank the ACE MAG and SWEPAM instrument teams and the ACE Science Center for providing the ACE data.

Topical Editor T. Pulkkinen thanks M. Bouhram and another referee for their help in evaluating this paper.

References

André, M. and Yau, A. W.: Theories and observations of ion energization and outflow in the high latitude magnetosphere, Space Sci. Rev., 80, 27–48, 1997.

Balogh, A., Carr, C. M., Acuna, M. H., Dunlop, M. W., Beek, T. J., Brown, P., Fornaon, K.-H., Georgescu, E., Glassmeier, K.-H., Harris, J., Musmann, G., Oddy, T., and Schwingenschuh, K.: The Cluster Magnetic Field Investigation: overview of in-flight performance and initial results, Ann. Geophys., 19, 1207–1217, 2001.

Bergmann, R., Roth, I., and Hudson, M. K.: Linear stability of the H^+- O^+ two-stream interaction in a magnetised plasma, J. Geophys. Res., 93, 4005–4020, 1988.

Bouhram, M., Malingre, M., Jasperse, J. R., and Dubouloz, N.: Modelling transverse heating and outflow of ionospheric ions from the dayside cusp/cleft, 1 A parametric study, Ann. Geophys., 21(8), 1753–1771, 2003a.

Bouhram, M., Malingre, M., Jasperse, J. R., Dubouloz, N., and Sauvaud, J.-A.: Modelling transverse heating and outflow of ionospheric ions from the dayside cusp/cleft, 2 Applications, Ann. Geophys., 21(8), 1773–1791, 2003b.

Chen, J. and Fritz, T. A.: Energetic oxygen ions of ionospheric origin observed in the cusp, Geophys. Res. Lett., 28, 1459–1462, 2001.

Cladis, J. B.: Parallel acceleration and transport of ions from polar ionosphere to plasmasheet, J. Geophys. Res., 13, 893–896, 1986.

Dubouloz, N., Delcourt, D., Malingre, M., Berthrlier, J.-J., and Chugunin, D.: Remote analysis of cleft ion acceleration using thermal plasma measurements from Interball Auroral Probe, Geophys. Res. Lett., 25, 2925–2928, 1998.

Dubouloz, N., Bouhram, M., Senior, C., Delcourt, D., Malingre, M., and Sauvaud, J.-A.: Spatial structure of the cusp/cleft ion fountain: A case study using a magnetic conjugacy between Interball AP and a pair of SuperDARN radars, J. Geophys. Res., 106, 261–274, 2001.

Gorney, D. J. A., Clarke, A., Croley, D., Fennell, J., and Luhmann, J.: The distribution of ion beams and conics below 8000 km, J. Geophys. Res., 86, 83–89, 1981.

Guglielmi, A. and Lundin, R.: Ponderomotive upward acceleration of ions by ion cyclotron and Alfvén waves over the polar regions, J. Geophys. Res., 106, 13 219–13 236, 2001.

Joko, S., Nilsson, H., Popielwaska, B., Rème, H., Bosqued, J.-M., Sauvaud, J.-A., Dandouras, I., Möbius, E., Kistler, L. M.,

Klecker, B., Carlson, C. W., McFadden, J. P., Parks, G. K., Bavassano-Cattaneo, M. B., Korth, A., Lundin, R., and Eliasson, L.: Shell-like configuration in O^+ ion velocity distribution at high altitudes in the dayside magnetosphere observed by CIS/Cluster, Ann. Geophys., in print, 2003b.

Krauklis, I., Johnstone, A. D., and Peterson, W. K.: Acceleration of ionospheric O^+ ions on open field lines in the Low-Latitude Boundary Layer and the cusp region, J. Geophys. Res., 106, 29 611–29 618, 2001.

Lockwood, M., Waite Jr., J. H., Moore, T. E., Johnson, J. F. E., and Chappell, C. R.: A new source of Suprathermal O^+ ions near the dayside polar cap boundary, J. Geophys. Res., 90, 4099–4116, 1985.

Ludlow, G. R. and Kaufman, R. L.: Heating of upflowing auroral H^+ and O^+ beams: results from quasi-linear theory, J. Geophys. Res., 94, 319–328, 1989.

Miyake, W., Mukai, T., and Kaya, N.: On the evolution of ion conics along the field line from EXOS D observations, J. Geophys. Res., 98, 11 127–11 134, 1993.

Moore, T. E., Lundin, R., Alcayde, D., André, M., Ganguli, S. B., Temerin, M., and Yau, A.: Source processes in the high-altitude ionosphere, Space Sci. Rev., 88, 7–84, 1999.

Nilsson, H., Yamauchi, M., Eliasson, L., Norberg, O., and Clemmons, J.: The ionospheric signature of the cusp as seen by incoherent scatter radar, J. Geophys. Res., 101, 10 947–10 963, 1996.

Ogawa, Y., Fujii, R., Buchert, S. C., Nozawa, S., and Ohtani, S.: Simultaneous EISCAT Svalbard radar and DMSP observations of ion upflow in the dayside polar ionosphere, J. Geophys. Res., 108, doi:10.1029/2002JA009590, 2003.

Paschmann, G. and Daly, P. E.: Analysis methods for multi spacecraft measurements, Kluwer Academic Publishers, 1998.

Rème, H., Aoustin, C., Bosqued, J. M., Dandouras, I., Lavraud, B., Sauvaud, J. A., Barthe, A., Bouyssou, J., Camus, T., Coeur-Joly, O., Cros, A., Cuvilo, J., Ducay, F., Garbarowitz, Y., Medale, J. L., Penou, E., Perrier, H., Romefort, D., Rouzaud, J., Vallat, C., Alcaydé, D., Jacquey, C., Mazelle, C., d'Uston, C., Möbius, E., Kistler, L. M., Crocker, K., Granoff, M., Mouikis, C., Popecki, M., Vosbury, M., Klecker, B., Hovestadt, D., Kucharek, H., Kuenneth, E., Paschmann, G., Scholer, M., Sckopke, N., Seidenschwang, E., Carlson, C. W., Curtis, D. W., Ingraham, C., Lin, R. P., McFadden, J. P., Parks, G. K., Phan, T., Formisano, V., Amata, E., Bavassano-Cattaneo, M. B., Baldetti, P., Bruno, R., Chionchio, G., Lellis, A. D., Marcucci, M. F., Pallocchia, G., Korth, A., Daly, P. W., Graeve, B., Rosenbauer, H., Vasyliunas, V., McCarthy, M., Wilber, M., Eliasson, L., Lundin, R., Olsen, S., Shelley, E. G., Fuselier, S., Ghielmetti, A. G., Lennartsson, W., Escoubet, C. P., Balsiger, H., Friedel, R., Cao, J.-B., Kovrazhkin, R. A., Papamastorakis, I., Pellat, R., Scudder, J., and Sonnerup, B.: First multispacecraft ion measurements in and near the Earth's magnetosphere with the identical Cluster ion spectrometry (CIS) experiment, Ann. Geophys., 19, 1303–1354, 2001.

Seki, K., Hirahara, M., Terasawa, T., Mukai, T., Saito, Y., Machida, S., Yamamoto, T., and Kokubun, S.: Statistical properties and possible supply mechanisms of tailward cold O^+ beams in the lobe/mantle regions, J. Geophys. Res., 103, 4477–4489, 1998.

Shelley, E., Johnson, R. G., and Sharp, R. D.: Satellite observations of energetic heavy ions during a geomagnetic storm, J. Geophys. Res., 77, 6104, 1972.

Valek, P. W., Perez, J. D., Jahn, J.-M., Pollock, C. J., Wüest, M. P., Friedel, R. H. W., Moore, T. E., and Peterson, W. K.: Outflow from the ionosphere in the vicinity of the cusp, J. Geophys. Res., 107, doi:10.1029/2001JA000107, 2002.

Yau, A. W. and André, M.: Sources of ion outflow in the high latitude ionosphere, Space Sci. Rev., 80, 1–25, 1997.

Yau, A. W., Whalen, B. A., Peterson, W. K., and Shelley, E. G.: Distribution of upflowing ionospheric ions in the high-altitude polar cap and auroral ionosphere, J. Geophys. Res., 89, 5507–5512, 1984.